The intriguing life of massive galaxies
Proceedings IAU Symposium No. 295, 2012
D. Thomas, A. Pasquali & I. Ferreras, eds.

doi:10.1017/S1743921313004511

Evolution of the most massive galaxies to $z \sim 0.6$

Yanmei Chen

Department of Astronomy, Nanjing University, Nanjing 210093, China
Key Laboratory of Modern Astronomy and Astrophysics, Ministry of Education, China
email: chenym@nju.edu.cn

Abstract. We develop a new method to estimate galaxy physical parameters, such as stellar masses, or star formation histories. This method is based on principal component analysis (PCA), using the information in rest-frame 3700-5500Å spectral region. The derived physical parameters are then applied to study the evolution of the most massive galaxies from $z \sim 0.6$ to the local Universe, especially on how radio AGN influence the recent star formation histories of host galaxies.

Keywords. galaxies: evolution - galaxies: star formation

1. Introduction

Over the last decades, several well-developed methods of estimating stellar mass (M_*) and star formation histories (SFH) were presented. For example, stellar mass-to-light ratio (M_*/L) can be derived from multi-band photometry (Brinchmann *et al.* 2004, Salim *et al.* 2005). If spectra are available, M_*/L and SFH can be derived from narrow band indices, D4000 and Hδ_A (Kauffmann *et al.* 2003) . Here come the questions: "why put our energy in developing a new method?", and "what's the advantage of this method?". The proposed new method (1) uses the full spectral region in rest-frame 3700-5500Å, which contains more information than in multi-band colors and in narrow band indices - which helps break degeneracies (e.g. age-dust, age-metallicity); (2) gives more robust galaxy parameters especially for low S/N data like the Baryon Oscillation Spectroscopic Survey (BOSS).

2. Overview

In the following, we will introduce the method of deriving physical parameters step by step. First, we build a model library of galaxies. The model library is parametrized as follows

(*a*) *SFHs.* Each SFH consists of three parts: a) an underlying continuous model, b) a series of super-imposed stochastic bursts, c) a random probability for star formation to stop exponentially (i.e. truncation).

(*b*) *Metallicity.* 95% of the model galaxies in our library are distributed uniformly in metallicity from $0.2-2.5Z_\odot$; 5% of the model galaxies are distributed uniformly between 0.02 and $0.2Z_\odot$.

(*c*) *Dust extinction.* Dust extinction is modelled using the two-component model described in Charlot & Fall (2000). The younger populations with age younger than 10^7yr, which live in birth clouds, suffer stronger dust extinction than the older populations.

Combining these parameters with the single stellar population model (Bruzual & Charlot 2003, Maraston & Stromback 2011), we build a library of 25,000 model spectra. Each

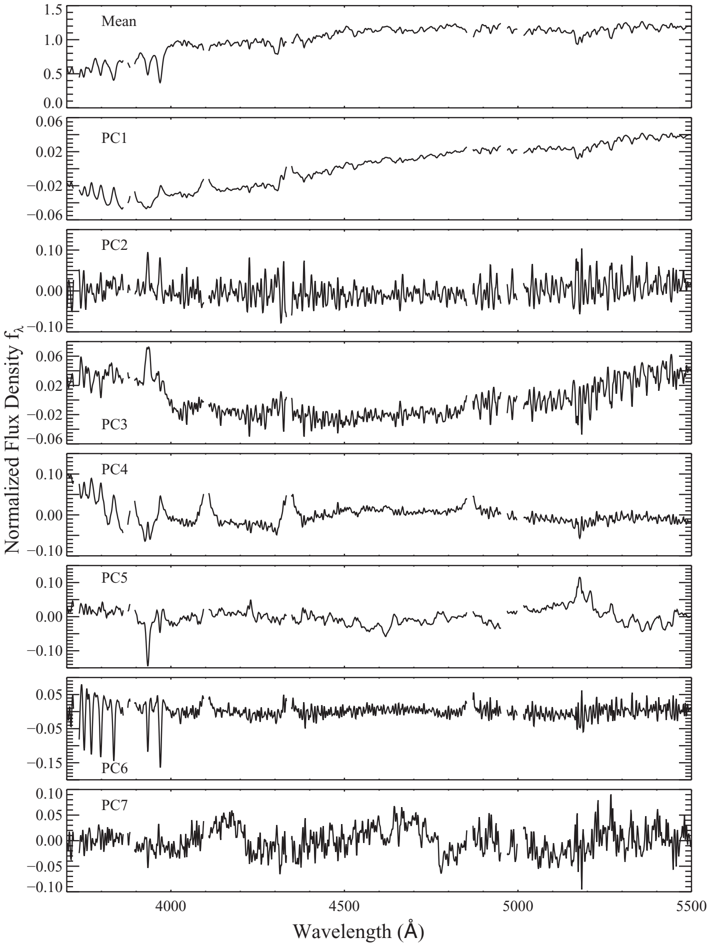

Figure 1. From top to bottom: the mean spectrum of the model library followed by the seven most significant eigenspectra.

of the model spectra is convolved to a velocity that is uniformly distributed over the range of values from 50 to 400 km s^{-1} to mimic stellar velocity dispersion.

Second, we run the PCA code on the model library to identify the significant principal components (PCs) of the spectral library. Figure 1 presents the mean spectrum and the first seven PCs for our input model library. As expected, the mean spectrum is typical of that of a galaxy with an intermediate age stellar population. The first PC provides a first-order measure of the age of the stellar population and it is strongly correlated with both 4000Å break and Balmer absorption line strengths. The second and third PC contain information about velocity dispersion and metallicity. The fourth PC clearly recovers information contained in the Balmer absorption lines. CaII (H+K) and Mgb absorption lines are clearly visible in the fifth PC, this component carries information about galaxy metallicity.

Third, we decompose each model and observed spectrum into its PC representation. Figure 2 is an example, the black spectrum is BOSS data, the red is the best fit. It is a linear combination of PCs:

$$S_\lambda = M_\lambda + \sum_\alpha C_\alpha \; E_{\alpha,\lambda}, \tag{2.1}$$

https://doi.org/10.1017/S1743921313004511 Published online by Cambridge University Press

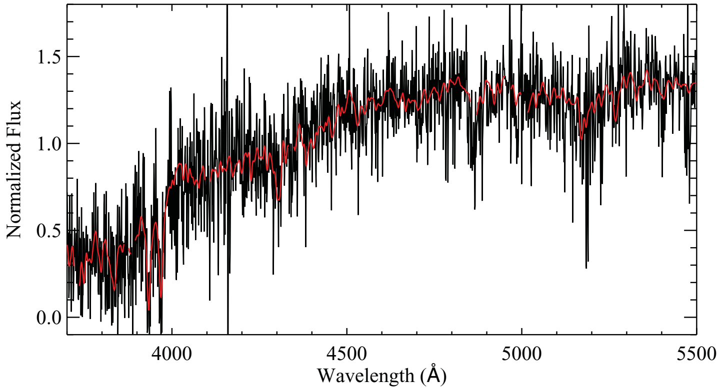

Figure 2. Example of the projection of a spectrum from BOSS data (black line) onto PCs (represented by the red central line).

where M_λ is the mean spectrum of the model library. C_α is the amplitude of the α-th PC $E_{\alpha,\lambda}$ (Note that α ranges from 1 to 7). Through this decomposition, we get the coefficient C_α.

Finally, in the seven-dimensional C_α space, the observed galaxy is a point. In the ideal case, the 25,000 models should be uniformly distributed in PC-space. Let's take the observed galaxy as the center, the errors of C_α as the radius in the seven-dimensional space. We get physical parameters of the observed galaxy by finding all the models located within the chosen radius, and assuming the physical parameters of the observed galaxy are similar to these models.

3. Implications

Evolution of the most massive galaxies to $z \sim 0.6$. We select a low-redshift galaxy sample from DR7: $14.5 < r < 17.6$, $0.055 < z < 0.3$ and a high-redshift sample from BOSS ("CMASS") with $0.55 < z < 0.7$. With the SFHs, we define a parameter, $F(> 10\%)$, fraction of galaxies with more than 10% of their stellar masses formed in the last Gyr. For simplicity, we will refer to it as the fraction of actively star-forming galaxies. The left panel of figure 3 shows how this fraction changes with stellar mass and redshift. Two conclusions from the left panel of figure 3: (1) the fraction of actively star-forming galaxies with $\log M_* > 11.4$ has evolved strongly since redshift 0.6; (2) at $z \sim 0.6$ the fraction of active star forming galaxies flattens above $\log M_* > 11.7$.

The link between radio AGN activity and star formation. We cross-match the SDSS DR7 (BOSS) spectroscopic galaxy sample with the FIRST and NVSS surveys to generate the low (high) redshift radio-loud AGN sample. Any galaxy that meets our radio flux cut is termed "radio-loud". We create samples of radio-quiet galaxies, which are matched as closely as possible to the radio-loud AGN hosts. For each galaxy in the radio-loud sample, we find another galaxy located in the FIRST and NVSS survey area without a radio detection that is closely matched in redshift ($|\Delta z| < 0.005$), stellar mass ($|\Delta \log M_*| < 0.05$), and velocity dispersion ($|\Delta\sigma_*| < 10$km s^{-1}). In order to study evolutionary effects, we finally match the DR7 and CMASS galaxies by stellar mass. The right panel of figure 3 shows the fraction of actively star forming galaxies as a function radio luminosity. Black lines show results for DR7 (low-z), while red lines are for CMASS (high-z). The dashed and solid lines represent the radio-loud galaxies and the radio-quiet controls, respectively. Note that for the radio-quiet galaxies, we use the radio luminosity from their radio-loud

https://doi.org/10.1017/S1743921313004511 Published online by Cambridge University Press

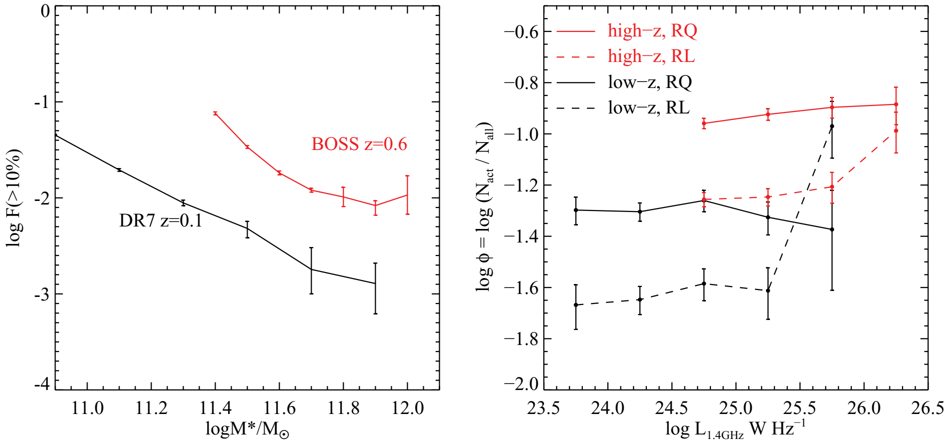

Figure 3. The left panel shows how this fraction of actively star forming galaxies changes with stellar mass and redshift; the right panel shows the fraction of actively star forming galaxies as a function radio luminosity. Black lines show results for DR7 (low-z), while red lines are for CMASS (high-z). The dashed and solid lines represent the radio-loud galaxies and the radio-quiet controls, respectively.

twins as the x-axis quantity. RL and RQ represent radio-loud and radio-quiet respectively. The main point of this plot is that the fraction of actively star forming galaxies is about 2 times higher in the radio quiet samples. This fraction remains constant over a wide range in radio luminosity. At the very highest radio luminosities, this fraction suddenly increases in radio loud samples.

References

Brinchmann, J., Charlot, S., White, S. D. M., Tremonti, C., Kauffmann, G., Heckman, T., & Brinkmann, J. 2004, *MNRAS*, 351, 1151

Bruzual, G. & Charlot, S. 2003, *MNRAS*, 344, 1000

Charlot, S. & Fall, S. M. 2000, *ApJ*, 539, 718

Chen, Y. M., Kauffmann, G., Tremonti, C. A., *et al.* 2012, *MNRAS*, 421, 314

Kauffmann, G., Heckman, T. M., White, S. D. M., *et al.* 2003, *MNRAS*, 341, 33

Maraston, C., & Stromback, G. 2011 *MNRAS*, 418, 2785

Salim, S., Charlot, S., Rich, R. M., *et al.* 2005, *ApJ*, 619, L39

https://doi.org/10.1017/S1743921313004511 Published online by Cambridge University Press